



## Article

# Damage Evaluation in Tempered Vacuum Glazing via Multivariate Statistical Methods

Xiaobo Xi <sup>1,\*</sup> , Jiawen Xu <sup>1</sup>, Jingyun Yuan <sup>2</sup>, Yifu Zhang <sup>1</sup> , Baofeng Zhang <sup>1</sup> and Ruihong Zhang <sup>1,\*</sup>

<sup>1</sup> School of Mechanical Engineering, Yangzhou University, Yangzhou 225127, China; 830108@njucm.edu.cn (J.X.); zyfu@yzu.edu.cn (Y.Z.); bf\_zhang@yzu.edu.cn (B.Z.)

<sup>2</sup> Yangzhou Institute of Technology, Yangzhou 225009, China; 101963@yzpc.edu.cn

\* Correspondence: xbxix@yzu.edu.cn (X.X.); zhangrh@yzu.edu.cn (R.Z.); Tel.: +86-0514-8797-8347 (X.X.)

**Abstract:** The performance of tempered vacuum glazing (TVG) strongly depends on the structural parameters and degree of damage of the products. In this paper, attention was paid to six performance indicators which had a major influence on the damage of TVG, and new evaluation parameters were derived from them using principal component analysis (PCA). In particular, hierarchical clustering analysis (HCA) based on Euclidean distance measurement enabled TVG products to be classified into three kinds. Considering the results of PCA, product quality classification was established according to the degree of damage. The evaluation method proposed in this work was found to be simple and reliable to provide references for damage detection of TVG.

**Keywords:** tempered vacuum glazing; glass damage; principal component analysis; hierarchical clustering analysis; evaluation model



**Citation:** Xi, X.; Xu, J.; Yuan, J.; Zhang, Y.; Zhang, B.; Zhang, R. Damage Evaluation in Tempered Vacuum Glazing via Multivariate Statistical Methods. *Appl. Sci.* **2021**, *11*, 4799. <https://doi.org/10.3390/app11114799>

Academic Editor: Luigi Biolzi

Received: 23 March 2021

Accepted: 22 May 2021

Published: 24 May 2021

**Publisher's Note:** MDPI stays neutral with regard to jurisdictional claims in published maps and institutional affiliations.



**Copyright:** © 2021 by the authors. Licensee MDPI, Basel, Switzerland. This article is an open access article distributed under the terms and conditions of the Creative Commons Attribution (CC BY) license (<https://creativecommons.org/licenses/by/4.0/>).

## 1. Introduction

Vacuum glazing is a high-quality product that possesses transparency, heat preservation, and sound insulation. Compared to insulating glass, vacuum glazing lasts longer and ensures the better heat transfer at a more compact design [1–3]. The manufacturing process of vacuum glazing is complex and needs two pieces of washed glass. First, support pillars are arranged in a specific manner on one piece of glass coated with an edge sealing solder. Another piece of glass is heat sealed and the space between both sheets of glass is afterwards evacuated with a vacuum pump [4–6]. However, low bend strength and impact toughness, as well as angular fragmentation after breaking, make vacuum glazing uncomfortable for safe use because of the risk of personal injury.

The mechanical strength and impact toughness can be enhanced by exposing one layer of tempered glass to the compressive surface stress and another layer to the interior tensile stress. Unlike the common glass, the bend strength of tempered glass can be increased by 3–5 times and the impact strength is enhanced by 5–10 times [7]. Meanwhile, the long-term medium-high temperature may cause the stress attenuation effect, and the glass performance will be degraded during the manufacturing process, which may affect the safe use of the product [8,9]. The common damage-inducing factors of TVG are surface stress, vacant pillars, sealing quality, and micro cracks. However, their industry-scale assessment with respect to product quality and eligibility is still a challenge [10–13].

In view of the complex quality parameters of TVG, one can mention a study of Hu D. et al. [14] who performed the grey relational analysis to study the module vacuum glass without, however, reporting the specific quality evaluation and the classification model. In that regard, this paper aims to evaluate the TVG performance by applying the multivariate statistical methods such as principal component analysis (PCA) and hierarchical component analysis (HCA). Both of these approaches are widely applied in the quality assessment related to food, medicine, wine, and other fields [15–17]. Attention is

paid to the development of the reliable evaluation model that would provide the references to product quality.

## 2. Materials and Methods

### 2.1. Samples

The TVG samples were produced at the laboratory of Yangzhou University from December 2019 to April 2020. The samples were sealed at low temperature and subquality products with surface cracks and internal leakage were removed in advance. For the sake of product structure and priority, six characteristic parameters closely related to TVG performance were selected with respect to the details provided in Table 1.

**Table 1.** Characteristic parameters and symbolic meanings of TVG.

Symbol	Meaning
$Z_1$	surface stress
$Z_2$	vacant pillars
$Z_3$	bubble size
$Z_4$	bubble quantity
$Z_5$	surface microcrack depth
$Z_6$	surface microcrack quantity

### 2.2. Testing Methods

#### 2.2.1. Surface Stress Evaluation Basis

A Glass Stress SCALP 05 portable intelligent stress measuring system was used for the surface stress and toughness testing of TVG, with 1–5 mm measurement thickness, more than 1.0 MPa measurement range and 0.1 MPa measurement accuracy. Because of the surface stress redistribution and stress concentration at the sealed edge, the stress measuring position was selected at the diagonal intersection point in the center of four pillars, as shown in Figure 1. The surface stress evaluation basis obtained in accordance with the stress characteristics of TVG is shown in Table 2.

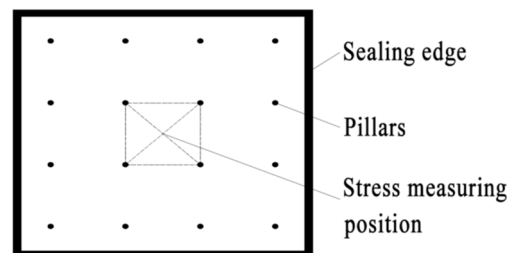


**Figure 1.** Schematic of a stress measuring position.

**Table 2.** Surface stress evaluation basis.

Evaluating Level	Evaluating Parameter	Surface Compressive Stress (MPa)
Excellent	8–10	$\geq 90$
Well	6–8	80–90
Poor	4–6	70–80
Worst	0–4	$< 70$

#### 2.2.2. Vacant Pillar Evaluation Basis

The incomplete support structure formed for vacant pillars which were caused by the pillar layout method or static electricity in the manufacturing process. Since the distance between the pillars would be larger than the design value, this improved the bend strength, and the supporting stress around the deficiency position increased accordingly, affecting the product safety. In this respect, the vacant pillars could be detected using the industrial

camera. The maximum supporting stress  $\sigma_{max}$  and maximum deflection  $\omega_{max}$  of TVG would be influenced by continuous vacant support pillars (CVSP). The evaluation data could be classified into different levels according to the degree of  $\sigma_{max}$  and  $\omega_{max}$  change based on the license definition conditions of TVG with CVSP [18], as shown in Table 3.

Table 3. Vacant Pillar Evaluation basis [18].

Evaluating Level	Evaluating Parameter	Different Positions of Vacant Pillars			Values of $\sigma_{max}$ and $\omega_{max}$
		In the Center	At the Edge	At the Corner	
Excellent	8~10	No more than 1 CVSP	No more than 2 CVSP parallel arrangement	No more than 1 CVSP	$\sigma_{max} \leq 80$ MPa, $\omega_{max} \leq 40$ mm
Well	6~8	2 CVSP	3 or 4 CVSP parallel arrangement; 2 CVSP vertical arrangement	No more than 4 CVSP linear arrangement	$80$ MPa < $\sigma_{max} \leq 90$ MPa $40$ mm < $\omega_{max} \leq 50$ mm
Poor	4~6	3 or 4 CVSP linear arrangement	3 or 4 CVSP vertical arrangement	3 CVSP L-shaped arrangement	$90$ MPa < $\sigma_{max} \leq 110$ MPa $50$ mm < $\omega_{max} \leq 70$ mm
Worst	0~4	Others	Others	Others	$\sigma_{max} > 110$ MPa, $\omega_{max} > 70$ mm

2.2.3. Sealing Quality Evaluation Basis

Associativity and air tightness were the main basis parameters for sealing edge quality evaluation of TVG. The sizes and number of bubbles could be assessed directly from a sealing edge, as shown in Figure 2. Bubbles would occur in a sealing solder because of the improper sealing technology, inappropriate mixture of the flux and solvent, and incorrect sealing temperature. Too many bubbles would influence the bond strength and even cause leakage at the sealing edge [19]. Meanwhile, the air tightness would be affected if external air entered into the vacuum layer between the bubbles. In this work, two evaluation parameters—bubble size (the largest bubble area) (see Table 4) and bubble quantity within 10 cm around the sealing edge (Table 5) were chosen for evaluation.

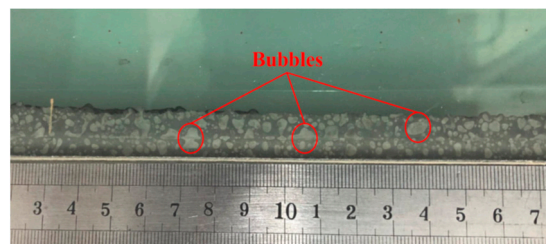


Figure 2. Bubbles in the sealing edge.

Table 4. Evaluation basis for bubble size at the sealing edge.

Evaluating Level	Evaluating Parameter	The Biggest Bubble Area (mm <sup>2</sup> )
Excellent	8–10	<5
Well	6–8	5–25
Poor	4–6	25–45
Worst	0–4	≥45

2.2.4. Evaluation Basis for Surface Microcracks

Micro-nickel sulfide stones existing in glass can cause a potential safety hazard [9,20]. In the sealing process of TVG, the heating temperature of 260 °C would promote the volume expansion of nickel sulfide particles with diameters of 0.04–0.65 mm, resulting in microcracks in the glass, which is a potential risk of self-explosion. Their surface was examined using an optical microscope and a three-dimensional profilometer. The main

parameters were the maximum crack depth and microcrack quantity within 1 mm<sup>2</sup>, as shown in Tables 6 and 7.

**Table 5.** Evaluation basis for bubble quantity at the sealing edge.

Evaluating Level	Evaluating Parameter	Bubble Quantity within 10 cm (Pieces)
Excellent	8–10	<150
Well	6–8	150–300
Poor	4–6	300–450
Worst	0–4	≥450

**Table 6.** Evaluation basis for surface microcrack depth.

Evaluating Level	Evaluating Parameter	Maximum Depth of Microcrack (µm)
Excellent	8–10	<0.1
Well	6–8	0.1–1
Poor	4–6	1–10
Worst	0–4	≥10

**Table 7.** Evaluation basis for surface microcrack quantity.

Evaluating Level	Evaluating Parameter	Microcrack Quantity within 1 mm <sup>2</sup> (Pieces)
Excellent	8–10	<200
Well	6–8	200–400
Poor	4–6	400–600
Worst	0–4	≥600

### 2.3. Evaluation Model

#### 2.3.1. Principal Component Analysis (PCA)

PCA is the method for finding the potential reigning factors in different related variables [21]. As a systematic product, characteristic parameters of TVG, such as surface microcracks and vacant pillars, have a close relationship between each other, exerting a direct influence on the surface stress. High multi-collinearity exists in different parameters, leading to incorrect regression equation parameters and even making the model unusable. PCA recombines original parameters to several aggregative indicators which not only provide more information but also have a poor linear relation due to the less information loss.

The standardized values of six characteristic parameters of TVG ( $Z_1, Z_2, \dots, Z_6$ ) are potential factors  $z_1, z_2, \dots, z_6$ . Assuming that six new coordinate axes  $p_i$  ( $i = 1, 2, \dots, 6$ ) have to be found in the original six-dimensional parameter space, the relationship between the original and new parameters can be expressed as follow:

$$\begin{cases} p_1 = b_{11}z_1 + b_{12}z_2 + \dots + b_{16}z_6 \\ p_2 = b_{21}z_1 + b_{22}z_2 + \dots + b_{26}z_6 \\ \dots \\ p_i = b_{i1}z_1 + b_{i2}z_2 + \dots + b_{i6}z_6 \end{cases} \quad (1)$$

Since these six parameters are related to each other, PCA allows one to find a lesser number of new variables to gather as much information as possible about the variance from the original variables. Therefore, these new variables are called principal components, and each of them is a linear combination of the original variables.

The maximum variance that can be found in the six orthogonal directions is presented by a feature vector and an eigenvalue. Both can be determined from the characteristic equation  $AZ = \lambda Z$ , where  $A$  is the covariance matrix of samples and  $\lambda$  represents the reassignment result for the total variance of the original variables in the principal components.

The distributive variance  $S_{p_i}$  of the  $i$ 'th principal component depends on the  $i$ 'th feature vector in the numerical data as follows:

$$S_{p_i} = \frac{\sum_{i=1}^6 (p_i - \bar{p}_i)^2}{n - 1} = \lambda_i \quad (2)$$

Given the contribution rate of each component, the total information can be expressed as follows:

$$m = \sum_{i=1}^6 \lambda_i \quad (3)$$

The feature vector is used to measure the information from the variables. In this respect, the contribution rate of each component can be found as:

$$\frac{\lambda_i}{\sum_{i=1}^6 \lambda_i} = \frac{S_{p_i}}{\sum_{i=1}^6 S_{p_i}} = \frac{\lambda_i}{m} \quad (4)$$

Therefore, the contribution rate of the  $k$ 'th component is:

$$\sum_{i=1}^k \frac{\lambda_i}{\sum_{i=1}^6 \lambda_i} = \sum_{i=1}^k \frac{\lambda_i}{m} \quad (5)$$

The pieces of principal components can be selected according to the contribution rate. In this study, we select the principal components whose  $\lambda$  is greater than one.

### 2.3.2. Hierarchical Clustering Analysis (HCA)

HCA is the multiple statistic method for solving classification problems in statistics [22]. In this approach, variable data in the unknown situation can be classified according to the intimacy degree characteristics. A basic idea of HCA is classifying things by distance or similarity. First, all things to be classified are considered as one kind, and their combination is then gradually made by distance or similarity. A large kind can be combined at last. Two-component data selected from the principal components of TVG create the two dimensional random vectors and bring them to the standardized form. A vector of  $n$  pieces of TVG is defined as:

$$\mathbf{u}_i = (x_{i1}, x_{i2}), i = 1, 2, \dots, n \quad (6)$$

The Euclidean distance  $D(a, b)$  is used to express the distance between the different samples  $i$  and  $j$  as follows:

$$D(\mathbf{u}_i, \mathbf{u}_j) = \sqrt{\sum_{k=1}^2 (x_{ik} - x_{jk})^2} \quad (7)$$

## 3. Results

### 3.1. Evaluation Data

Thirteen pieces of TVG were randomly chosen to test the above described six parameters. The evaluation parameters were given according to Tables 2–7. The testing results are shown in Table 8.

**Table 8.** Testing results of characteristic parameters of TVG.

Sample	Z <sub>1</sub>	Z <sub>2</sub>	Z <sub>3</sub>	Z <sub>4</sub>	Z <sub>5</sub>	Z <sub>6</sub>
1	9	9	8	9	7	8
2	7	8	7	9	8	9
3	7	8	6	7	8	8
4	8	9	8	7	8	7
5	8	8	7	5	7	7
6	7	7	6	5	6	7
7	8	9	9	7	7	8
8	7	6	8	7	7	7
9	7	7	8	5	8	8
10	7	8	7	7	6	7
11	8	8	8	7	8	9
12	8	9	8	9	8	7
13	9	8	8	9	7	8

### 3.2. PCA Process and Results

To standardize data in Table 8, average values and standard deviations were calculated at first (see Table 9). After that the data were standardized using the normalization method. The results can be seen in Table 10.

**Table 9.** Average values and standard deviations of sample parameters.

Parameter	Average Value	Standard Deviation
Z <sub>1</sub>	7.69	0.751
Z <sub>2</sub>	8	0.913
Z <sub>3</sub>	7.54	0.877
Z <sub>4</sub>	7.15	1.519
Z <sub>5</sub>	7.31	0.751
Z <sub>6</sub>	7.69	0.751

**Table 10.** Standardized results of sample parameters.

Sample	z <sub>1</sub>	z <sub>2</sub>	z <sub>3</sub>	z <sub>4</sub>	z <sub>5</sub>	z <sub>6</sub>
1	1.74111	1.09545	0.52623	1.21529	−0.40967	0.40967
2	−0.92176	0	−0.61394	1.21529	0.92176	1.74111
3	−0.92176	0	−1.75412	−0.10127	0.92176	0.40967
4	0.40967	1.09545	0.52623	−0.10127	0.92176	−0.92176
5	0.40967	0	−0.61394	−1.41784	−0.40967	−0.92176
6	−0.92176	−1.09545	−1.75412	−1.41784	−1.74111	−0.92176
7	0.40967	1.09545	1.66641	−0.10127	−0.40967	0.40967
8	−0.92176	−2.19089	0.52623	−0.10127	−0.40967	−0.92176
9	−0.92176	−1.09545	0.52623	−1.41784	0.92176	0.40967
10	−0.92176	0	−0.61394	−0.10127	−1.74111	−0.92176
11	0.40967	0	0.52623	−0.10127	0.92176	1.74111
12	0.40967	1.09545	0.52623	1.21529	0.92176	−0.92176
13	1.74111	0	0.52623	1.21529	−0.40967	0.40967

PCA was performed afterwards on the data from Table 10 using Statistical Product and Service Solutions (SPSS) software, and the results are shown in Table 11. Six components were selected from the initial solution. The total variance of the original variables was calculated, giving the cumulative contribution rate of 100%. Two components with  $\lambda$  exceeding one (2.607 and 1.314) were selected as the most informative, whose contribution rates were found to be 43.455% and 21.906%, respectively, resulting in the cumulative contribution rate of 65.361%. In this case, PCA is satisfactory because most of the information about the parameters of the samples could be successfully extracted.

**Table 11.** Variance expression of major parameters from PCA.

Element	$\lambda$	Contribution Rate (%)	Cumulative Contribution Rate (%)
1	2.607	43.455	43.455
2	1.314	21.906	65.361
3	0.751	12.51	77.871
4	0.613	10.214	88.085
5	0.451	7.509	95.594
6	0.264	4.406	100

The coefficients of elements 1 and 2 were afterwards calculated using the regression method in SPSS software. The results are available in Table 12, where  $z_1$  and  $z_2$  components account for a major proportion. This means that surface stress and vacant pillars exert a significant influence on the TVG damage, which agrees with a practical situation.

**Table 12.** Element coefficients.

Parameter	Element 1	Element 2
$z_1$	0.424	−0.184
$z_2$	0.347	−0.046
$z_3$	0.288	−0.012
$z_4$	0.255	0.138
$z_5$	−0.076	0.556
$z_6$	−0.085	0.565

According to the data in Table 12 and Formula (1), the new variables were determined as follows:

$$\begin{cases} p_1 = 0.424z_1 + 0.347z_2 + 0.288z_3 + 0.255z_4 - 0.076z_5 - 0.085z_6 \\ p_2 = -0.184z_1 - 0.046z_2 - 0.012z_3 + 0.138z_4 + 0.556z_5 + 0.565z_6 \end{cases} \quad (8)$$

In turn, the scores of two principal components were generated by calculating the standardized values from Table 10 using Formula (8). The results can be found in Table 13.

**Table 13.** PCA scores.

Sample	Element 1	Element 2
1	1.57675	−0.20624
2	−0.47615	1.83955
3	−1.02674	0.92008
4	0.68759	−0.15389
5	−0.25445	−1.01149
6	−1.42654	−1.44314
7	1.00464	−0.15629
8	−0.91717	−0.49734
9	−1.086	0.76275
10	−0.38296	−1.32612
11	0.082	1.40016
12	1.02268	0.02739
13	1.19635	−0.15542

### 3.3. HCA Process and Results

HCA was applied to the damage-inducing parameters of thirteen TVG pieces by using SPSS software. Table 14 shows the Euclidean distances between the samples. The first minimum Euclidean distance (0.168) was found for samples 3 and 9, meaning that. According to HCA, these can be classified into one kind. The next Euclidean distance (0.185) linked samples 7 and 12.



**Table 14.** Matrix of Euclidean distances between each sample.

Sample	Euclidean Distance												
	1	2	3	4	5	6	7	8	9	10	11	12	13
1	0	2.898	2.837	0.891	2	3.248	0.574	2.511	2.834	2.257	2.194	0.601	0.384
2	2.898	0	1.072	2.308	2.86	3.417	2.485	2.378	1.237	3.167	0.71	2.352	2.603
3	2.837	1.072	0	2.023	2.08	2.397	2.299	1.422	0.168	2.337	1.208	2.235	2.47
4	0.891	2.308	2.023	0	1.274	2.476	0.317	1.641	1.996	1.588	1.668	0.381	0.509
5	2	2.86	2.08	1.274	0	1.249	1.522	0.839	1.959	0.34	2.435	1.646	1.685
6	3.248	3.417	2.397	2.476	1.249	0	2.751	1.074	2.232	1.05	3.219	2.857	2.922
7	0.574	2.485	2.299	0.317	1.522	2.751	0	1.952	2.284	1.815	1.809	0.185	0.192
8	2.511	2.378	1.422	1.641	0.839	1.074	1.952	0	1.271	0.986	2.144	2.01	2.141
9	2.834	1.237	0.168	1.996	1.959	2.232	2.284	1.271	0	2.204	1.331	2.233	2.46
10	2.257	3.167	2.337	1.588	0.34	1.05	1.815	0.986	2.204	0	2.766	1.951	1.966
11	2.194	0.71	1.208	1.668	2.435	3.219	1.809	2.144	1.331	2.766	0	1.664	1.914
12	0.601	2.352	2.235	0.381	1.646	2.857	0.185	2.01	2.233	1.951	1.664	0	0.252
13	0.384	2.603	2.47	0.509	1.685	2.922	0.192	2.141	2.46	1.966	1.914	0.252	0

Table 15 depicts the condensation states of all TVG samples, and the connection statistics between Clusters 1 and 2 were used for clustering. Based on the results from Table 14, samples 3 and 9 were clustered into one kind with a coefficient of 0.168. Another clustering occurred between samples 7 and 12 with a coefficient of 0.185. The next possible clustering was between samples 7 and 13 as sample 13 joined with sample 7 and sample 12, with the coefficients of 0.192, and so on.

**Table 15.** Condensation states of TVG samples.

Stage	Clustering Combination		Coefficient	First Appeared Order Cluster		Next Stage
	Cluster 1	Cluster 2		Cluster 1	Cluster 2	
1	3	9	0.168	0	0	10
2	7	12	0.185	0	0	3
3	7	13	0.192	2	0	5
4	5	10	0.34	0	0	8
5	4	7	0.317	0	3	6
6	1	4	0.891	0	5	11
7	2	11	0.71	0	0	10
8	5	8	0.839	4	0	9
9	5	6	1.249	8	0	11
10	2	3	1.072	7	1	12
11	1	5	2	6	9	12
12	1	2	2.898	11	10	0

Figure 3 shows a tree diagram as a result of HCA of the selected data. The distances between different kinds were mapped in accordance with numbers 0 to 25. As expected, the samples could be classified into the three groups, if drawing a line at a point 15 on the abscissa. The first kind composed samples 3, 9, 2, and 11. The second was formed by sample 7, 12, 13, 4, and 1, and the third one corresponded to sample 5, 8, 10, and 6.

It is noteworthy that the groups presented above were obtained according to the distances between the corresponding clusters only. In this respect, it is difficult to say which of the kinds is the best. To perform the quality analysis of the data, PCA was involved in the discussion. As seen in Table 11, the contribution rate of element 1 was obviously the largest, followed by that of element 2. The analysis of scores from Table 13 for each sample at elements 1 and 2 revealed that element 1 including samples 7, 12, 13, 4, and 1 got the highest score of 0.68759 and even more, which indicated the highest quality as a whole. In turn, the lower scores of the group including samples 3, 9, 2, and 11 and the kind formed by samples 5, 10, 8, and 6 meant the lower quality. However, distinguishing



the better group among the latter two kinds is a challenge that requires a further analysis of element 2. While the scores of the group including samples 3, 9, 2, and 11 are above zero, those of the kind with samples 5, 10, 8, and 6 are below zero. Therefore, the quality of the former kind of samples is better. The relevant grade classification of TVG can be found in Table 16.

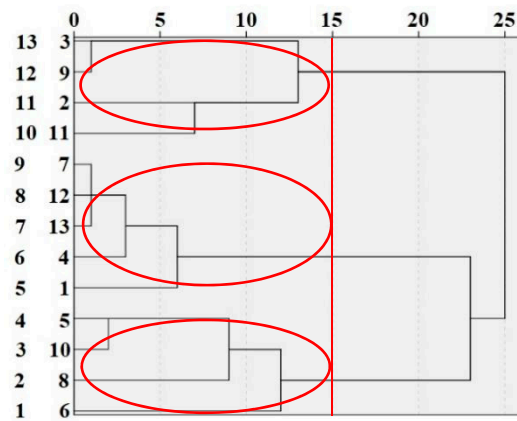


Figure 3. Tree diagram as a result of HCA.

Table 16. Grade classification of TVG.

Grade	Grade Meaning	Corresponding Sample Number
Grade I	Minor damage	1, 4, 7, 12, 13
Grade II	Mediate damage	2, 3, 9, 11
Grade III	Serious damage	5, 6, 8, 10

Besides, the average values on elements 1 and 2 of the corresponding samples were calculated with respect to the three grades of damage, and the results are shown in Table 17.

Table 17. Average values for two principal components of each grade.

Grade	Sample Number	Average Value of Element 1	Average Value of Element 2
Grade I	5	1.09760	−0.12889
Grade II	4	−0.62672	1.23063
Grade III	4	−0.74528	−1.06952

In this respect, evaluating the performance of new TVGs can be implemented through the calculation of Euclidean distances of sample’s two principal components and their average values. Each minimum Euclidean distance between the samples allows them to be automatically classified into a certain kind.

### 3.4. Evaluation Model Verification

The damage evaluation model of TVG can be summarized according to the evaluation process described above. First, six characteristic parameters were tested for the new samples. Each parameter was then standardized and two principal components were found. After that, Euclidean distances of the average values were calculated for main components, allowing one to extract various grades of the samples. Finally, the sample grade could be classified into the kinds with the minimum distance. The whole process of evaluation and verification is shown in Figure 4.

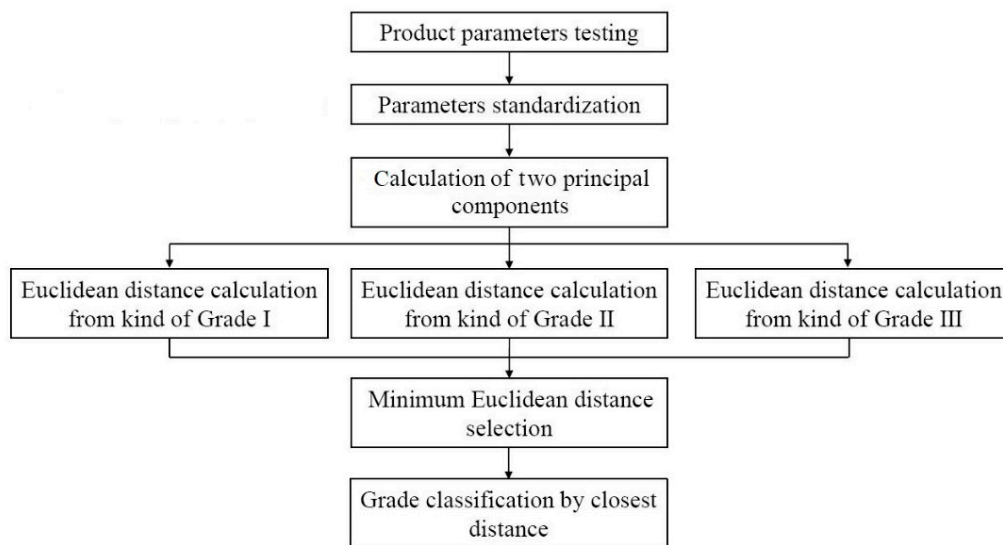


**Figure 4.** Flow chart for model verification.

Taking a new sample of TVG and testing six characteristic parameters result in:  $Z_1 = 8$ ,  $Z_2 = 9$ ,  $Z_3 = 7$ ,  $Z_4 = 7$ ,  $Z_5 = 8$ , and  $Z_6 = 8$ . Standardizing them using data in Table 9 provides the values:  $z_1 = 0.41278$ ,  $z_2 = 1.09529$ ,  $z_3 = -0.61574$ ,  $z_4 = -0.09875$ ,  $z_5 = 0.91877$ , and  $z_6 = 0.41279$ . Putting them into Formula (8) gives two principal components as  $p_1 = 0.24766$ ,  $p_2 = -0.61149$ . Applying Formula (7) ensures Euclidean distances between the new samples' principal components and the corresponding average values from Table 17, and the results can be found in Table 18. According to these data, the new sample is close to Grade I and can thereby be classified with respect to this grade.

**Table 18.** Euclidean distances between new samples' principal components and the average values for each grade.

Grade	Euclidean Distance
Grade I	1.12719
Grade II	1.17630
Grade III	1.95236

#### 4. Conclusions

The damage evaluation method of TVG was proposed based on the PCA and HCA multivariate statistical techniques. Six major characteristic parameters associated with the TVG damage were adopted and the evaluation parameters as the performance indicators were specified as well. In particular, PCA of six characteristic parameters enabled one to establish that surface stress and vacant pillars had a significant influence on the damage of TVG. Two new evaluation parameters, being in the linear correlation with original variable parameters, were created as well. The calculation of Euclidean distances through HCA of data allowed TVG to be classified into the three kinds with respect to the degree of damage. The evaluation method developed in this work was shown to be simple and reliable, providing references for damage detection of TVG and product quality improvement strategy.

**Author Contributions:** Conceptualization, X.X., J.X. and J.Y.; methodology, X.X., J.X. and J.Y.; software, X.X., J.X. and J.Y.; data curation, X.X., J.X. and J.Y.; formal analysis, Y.Z.; validation, B.Z.; writing—review and editing, R.Z.; funding acquisition, R.Z. All authors have read and agreed to the published version of the manuscript.

**Funding:** This research was funded by the National Natural Science Foundation of China (Grants Nos. 51772264 and 51902284), the Science and Technology Project of Yangzhou City (YZ2020017) and the Science and Technology Innovation Cultivation Fund Project of Yangzhou University (2019CXJ050).

**Institutional Review Board Statement:** Not applicable.

**Informed Consent Statement:** Informed consent was obtained from all subjects involved in the study.

**Data Availability Statement:** The data presented in this study are available on request from the corresponding author.

**Conflicts of Interest:** The authors declare no conflict of interest.

## References

1. Miao, H.; Shan, X.; Zhang, J.; Sun, J.; Wang, H. Effect of sealing temperature on the sealing edge performance of vacuum glazing. *Vacuum* **2015**, *116*, 7–12. [[CrossRef](#)]
2. Zhang, J.; Liu, S.; Zhang, Y.; Miao, H.; Zhang, S.; Zhang, Q. Formation mechanism of sealing edge pores for vacuum glazing using laser brazing technique. *Vacuum* **2018**, *147*, 1–7. [[CrossRef](#)]
3. Fang, Y.; Eames, P.C.; Norton, B. Effect of glass thickness on the thermal performance of evacuated glazing. *Sol. Energy* **2007**, *81*, 395–404. [[CrossRef](#)]
4. Collins, R.E.; Robinson, S.J. Evacuated glazing. *Sol. Energy* **1991**, *47*, 27–38. [[CrossRef](#)]
5. Collins, R.E.; Fischer-Cripps, A.C.; Tang, J.Z. Transparent evacuated insulation. *Sol. Energy* **1992**, *49*, 333–350. [[CrossRef](#)]
6. Zhu, Q.; Wu, W.; Yang, Y.; Han, Z.; Bao, Y. Finite element analysis of heat transfer performance of vacuum glazing with low-emittance coatings by using ANSYS. *Energy Build.* **2020**, *206*, 109584. [[CrossRef](#)]
7. Tang, J. *Vacuum Glazing*; Wuhan University of Technology Press: Wuhan, China, 2018.
8. Bishopa, D.W.; Thomasa, P.S.; Raya, A.S. Micro Raman characterization of nickel sulfide inclusions in toughened glass. *Mater. Res. Bull.* **2010**, *35*, 1123–1128. [[CrossRef](#)]
9. Sanya, O.T.; Owoeye, S.S.; Ajayi, O.J. Influence of chemical treatment on microstructure and mechanical properties of chemically-toughened glass by ion exchange process. *J. Non-Cryst. Solids* **2018**, *494*, 9–12. [[CrossRef](#)]
10. Wilson, C.F.; Simko, T.M.; Collins, R.E. Heat conduction through the support pillars in vacuum glazing. *Sol. Energy* **1998**, *63*, 393–406. [[CrossRef](#)]
11. Ng, N.; Collins, R.E.; So, L. Characterization of the thermal insulating properties of vacuum glazing. *Mater. Sci. Eng. B* **2007**, *138*, 128–134. [[CrossRef](#)]
12. So, L.; Ng, N.; Bilek, M. Analysis of the internal glass surfaces of vacuum glazing. *Mater. Sci. Eng. B* **2007**, *138*, 135–138. [[CrossRef](#)]
13. Griffiths, P.W.; Eames, P.C.; Hyde, T.J.; Fang, Y.; Norton, B. Experimental characterization and detailed performance prediction of a vacuum glazing system fabricated with a low temperature metal edge seal, using a validated computer model. *J. Sol. Energy Eng.* **2006**, *128*, 199–203. [[CrossRef](#)]
14. Hu, D.; Liu, C.; Li, Y. Reliability Analysis of toughened vacuum glass based on gray relation decision. *Math. Probl. Eng.* **2018**, *2018*, 2926480. [[CrossRef](#)]
15. Xue, Y.; Yu, H.; Zhang, P.; Li, J. Multivariate statistical analysis to evaluate the effects of different treatments on the shelf quality of blueberries. *Mod. Food Sci. Technol.* **2020**, *36*, 1–10.
16. Song, X.; Yuan, R.; Xu, J.; Zhang, C.; Zhang, X.; Sun, X. Comparative study on four vinegar processing methods of cyperi rhizoma based on multivariate statistical analysis. *J. Chin. Med. Mater.* **2020**, *43*, 842–846.
17. Li, H.; Liu, Y.; Guo, A.; Liang, X.; Kang, W.; Tao, Y. Sensory characteristic descriptor determination of wine by the polyphyletic statistical analysis. *J. Chin. Inst. Food Sci. Technol.* **2007**, *7*, 114–119.
18. Xi, X.; Shi, Y.; Shan, X.; Zhang, Y.; Shen, H.; Zhang, R. Mechanical properties of tempered vacuum glazing with vacant support pillars. *Vacuum* **2021**, *188*, 110165. [[CrossRef](#)]
19. Zhang, S.; Li, C.; Miao, H.; He, Q. The influence of welding process parameters on pore formation in pulsed laser-welded vacuum plate glazing. *Materials* **2019**, *12*, 1790. [[CrossRef](#)]
20. Bao, Y.; Liu, Z. Mechanism and criterion of spontaneous breakage of tempered glass. *J. Inorg. Mater.* **2016**, *31*, 401–406.
21. Lin, H.; Li, H.; Shao, G.; Ye, Y.; Yang, Y. Zero-point fault detection of load cells in truck scale based on recursive principal component analysis and comprehensive evaluation method. *Measurement* **2020**, *159*, 107706. [[CrossRef](#)]
22. Wang, R.; Fung, B.C.M.; Zhu, Y. Heterogeneous data release for cluster analysis with differential privacy. *Knowl. Based Syst.* **2020**, *201–202*, 106047. [[CrossRef](#)]